MATHEMATICAL BIOSCIENCES
AND ENGINEERING
Volume **7**, Number **2**, April **2010**

doi:10.3934/mbe.2010.7.363

pp. **363–384**

MATHEMATICALLY MODELING PCR: AN ASYMPTOTIC APPROXIMATION WITH POTENTIAL FOR OPTIMIZATION

Martha Garlick and James Powell

Department of Mathematics and Statistics
Utah State University, Logan UT 84322, USA

David Eyre and Thomas Robbins

Idaho Technology Inc.
390 Wakara Way, Salt Lake City UT 84108, USA

(Communicated by Sergei Pilyugin)

Abstract. A mathematical model for PCR (Polymerase Chain Reaction) is developed using the law of mass action and simplifying assumptions regarding the structure of the reactions. Differential equations are written from the chemical equations, preserving the detail of the complementary DNA single strand being extended one base pair at a time. The equations for the annealing stage are solved analytically. The method of multiple scales is used to approximate solutions for the extension stage, and a map is developed from the solutions to simulate PCR. The map recreates observed PCR well, and gives us the ability to optimize the PCR process. Our results suggest that dynamically optimizing the extension and annealing stages of individual samples may significantly reduce the total time for a PCR run. Moreover, we present a nearly optimal design that functions almost as well and does not depend on the specifics of a single reaction, and so would work for multi sample and multiplex applications.

1. **Introduction.** The Polymerase Chain Reaction (PCR) is a technique for enzymatic amplification of specific segments of DNA. Since its inception [11], it has revolutionized research involving genomic material. Pathogen detection, disease diagnosis, human genetics and developmental biology are just a few of the research areas impacted by PCR [12].

PCR is performed by repeating three temperature-induced stages: dissociation, annealing, and extension. In dissociation a sample containing the target DNA is first heated to approximately 95^oC to separate the DNA into single strands. The mixture is then cooled to allow primers to anneal to the template DNA. Primers are short single strands of DNA specifically designed to target and bracket the sequence of DNA in the sample to be duplicated (the amplicon). The temperature of this stage is primer-specific, ranging from 37^oC to 72^oC. The solution is then heated to 74^oC for extension. During this phase the thermostable enzyme Taq Polymerase synthesizes a new DNA strand, completing the complimentary sequence started by the primer. These three stages are repeated 30 to 45 times yielding millions of copies

2000 *Mathematics Subject Classification.* Primary: 74G10, 92C45.

Key words and phrases. PCR, polymerase chain reaction, dynamical systems, mathematical model, method of multiple scales, optimization.

of the target DNA [12]. In real world PCR, annealing and extension often overlap, so that extension of a strand begins immediately after it is primed. Therefore, in practice, only two temperatures may be used. To simplify modeling we consider the annealing and extension stages as two distinct and separate reactions; we will show below that this simplification maintains fidelity with real PCR.

Real-time PCR uses fluorescent probes to monitor the amplification of DNA throughout the reaction. The speed at which the fluorescent signal reaches a threshold level correlates with the amount of target DNA in the initial sample. Real-time PCR is used to precisely distinguish and measure concentrations of specific DNA sequences even if there is only a very small quantity present in the original sample [14]. This technology has many applications, including those that benefit from rapidity. Identification of microbes or parasites in commercial food and municipal water supplies, pathogen detection, and forensic applications are just a few. Portable, rapid, real-time PCR machines can determine the presence of a pathogen, such as anthrax, in as little as 30 minutes. However, 30 minutes can be a long time on a battlefield, in the event of a biological terror attack, or for a patient in the emergency room. Using mathematics to optimize the process to reduce this time is therefore a valuable exercise.

Idaho Technology Inc. of Salt Lake City UT develops and produces fast, high quality PCR machines for pathogen identification and DNA analysis. Beginning in the early 1990's in a corner of an agricultural business in Idaho Falls ID, they are now industry leaders in real-time PCR technology. They have funded research collaborations with the Department of Mathematics and Statistics at Utah State University for many years, aimed at process improvement. The research presented here is a response to their challenge to mathematically model the dynamics of Taq extending the DNA template one nucleotide base pair at a time, and evaluate possible process controls using that model.

PCR has been mathematically modeled in several different ways. Early models assumed growth per cycle proportional to the amplicon density. However, assuming exponential growth of template copies greatly oversimplifies the process and models the growth only for the first few cycles. In reality, limiting factors cause the process to slow and eventually stop. These factors may include exhaustion of primer molecules and raw base pairs or a decrease in the effectiveness of Taq [7].

In consideration of this limiting behavior, several mathematical models in the literature predict the efficiency of the PCR process. Liu and Saint [7] used a sigmoidal mathematical model to fit real time PCR data, and demonstrated that amplification efficiency can change from cycle to cycle. A linear regression approach to calculating PCR efficiency was given by Ramakers et al. [9], and Rutledge [10] proposed a simplified method for absolute quantification. Gevertz et al. [2] considered the efficiency of the reaction as a function of the cycle number. They considered an equilibrium model as well as a kinetic model by deriving differential equations directly from the chemical equations for the annealing and extension phases. Aach and Church [1] also derived mathematical equations from the chemical reactions, but for diffusion-constrained PCR reactions.

Stochastic and probabilistic models are also used to describe PCR. Velikanov and Kapral [15] treated the extension step as a microscopic Markov process in which the nucleotides bind onto the primed single strand of DNA one at a time. Sun et al. [13] used the theory of branching processes to develop a model for distributions of mutations and estimation of mutation rates during PCR. Weiss and Von Hessler

[16] treated the accumulation of new molecules during PCR as a random bifurcation tree to estimate overall error rates for the reaction. More recently, Jagers, et al. [4] used Galton-Watson branching processes to arrive at a linear growth phase following the initial exponential phase. Lalam [6] based another model on a Galton-Watson branching process description of PCR to estimate the reaction efficiency. A drawback of many of these models, particularly from the standpoint of optimization, is their complexity, which requires numerical integration and obscures dynamical understanding of the process.

The model we present uses the chemical reactions of PCR to derive a system of differential equations, mimicking the physical behavior of the single-stranded DNA (ssDNA) copy being extended one nucleotide base pair at a time. Addition of individual nucleotides occurs very rapidly, and the amount of Taq is small relative to both primer and base pair concentration. This provides leverage to apply an asymptotic solution strategy. There are two main objectives for the solution strategy for this mathematical model. First, the approximate solutions found by a multiple time scale approach can be put into a map to simulate the PCR process. Second, the solutions and the map can be used to optimize the time spent in each stage in order to obtain the most amplification in the shortest possible time. Our results indicate that dynamic optimizing of the extension and annealing phases may significantly decrease the time required for the entire PCR process. Moreover, we present a nearly optimal design that functions just as well and does not depend on the specifics of a single reaction.

2. **The chemical reactions of PCR.**

2.1. **Dissociation.** Dissociation occurs when the sample containing the double-stranded DNA (dsDNA) is heated to separate the dsDNA into single strands. The chemical equation can be written

$$D \rightarrow 2S,$$

where D is dsDNA and S is single-stranded DNA (ssDNA). Experimentation has shown that dsDNA held at temperatures above 94^oC for more that five seconds is completely denatured [2]. This justifies the assumption that dissociation is complete. Using lower case letters to indicate concentrations ($s = [S], d = [D]$), we represent this stage mathematically by $s = 2d$.

2.2. **Annealing.** After the dsDNA is denatured, two complementary ssDNA templates are formed. A primer is designed to anneal at the end of the target DNA template for each of the two complementary strands. We simplify the reaction by including only one chemical equation for this, assuming that the priming for each of the complementary strands occurs at the same rate. The chemical equation for annealing describes the primer, P, attaching to the ssDNA, S, to form a molecule of primed ssDNA, S', and is written

$$S + P \overset{k_1, k_{-1}}{\longleftrightarrow} S'.$$

The constant k_1 is the rate the reaction moves forward, creating primed ssDNA. A constant k_{-1} is included to model the reverse reaction of primers falling off of previously primed ssDNA. Reaction temperatures are chosen so that $k_1 >> k_{-1}$, allowing the reaction to proceed rapidly.

Other reactions can occur during annealing. The two complementary template strands can reanneal and primers can anneal to each other instead of to the ssDNA.

Since the length of the strand is generally greater than 100 base pairs, reannealing of the complementary templates is unlikely and we choose to neglect it. We also neglect the scenario of primer to primer annealing, since tremendous effort is exerted in primer design to prevent this.

2.3. **Extension.** In the extension stage, Taq polymerase, Q, binds with primed ssDNA, S', to form a complex, C, at the rate λ_1,

$$S' + Q \xrightarrow{\lambda_1} C.$$

Taq facilitates the addition of base pairs in order from the primer to the end of the strand. We write a separate equation for each base pair added; C_j denotes the complex with j base pairs ($j = 1, ..., n$). The number, n, denotes the number of nucleotide base pairs needed to complete the complementary strand and R represents the resources containing all 4 types of individual base pairs for extension. We assume that all base pairs add on to the template at the same rate, λ_2, and that all are present and needed in equal proportions. This assumption turns out to be less important than that the concentration of single nucleotide base pairs is overall quite high, as will be seen below.

The equations for this process are as follows:

$$\begin{gathered} C + R \xrightarrow{\lambda_2} C_1, \\ C_1 + R \xrightarrow{\lambda_2} C_2, \\ \vdots \\ C_{n-1} + R \xrightarrow{\lambda_2} C_n. \end{gathered}$$

The Taq separates from the dsDNA as the template copy is completed at the rate λ_3,

$$C_n \xrightarrow{\lambda_3} D + Q.$$

At the reaction temperatures used for PCR, Taq is quite efficient at synthesizing the complementary strands. Therefore, we consider any back reactions in this stage to be negligible. Descriptions of the reactants and constants are shown in Table 1.

3. Model development.

3.1. **Annealing.** The law of mass action is invoked to write a system of differential equations for the annealing stage of a single cycle of PCR. This approach is particularly well-justified in the case of quantitative PCR where reactions occur in small, well-mixed containers.

$$\frac{ds}{dt} = -k_1 sp + k_{-1} s', \tag{1}$$

$$\frac{dp}{dt} = -k_1 sp + k_{-1} s', \tag{2}$$

and

$$\frac{ds'}{dt} = k_1 sp - k_{-1} s'. \tag{3}$$

Equation (1) represents the change in the concentration of ssDNA as a function of the concentrations of ssDNA s, primer,p, and primed ssDNA, s', scaled by the forward and backward reaction rates, k_1 and k_{-1}. Likewise, equations (2) and (3) describe the change in concentration of primer and primed ssDNA. The initial conditions are $s'(0) = 0$ (since no primed ssDNA survives denaturing), $s(0) = \hat{s}$ (the

Symbols	Description
D, d	double stranded DNA (dsDNA), $d = [D]$ (concentration)
S, s	single stranded DNA (ssDNA), $s = [S]$
P, p	primer, $p = [P]$
S', s'	primed ssDNA, $s' = [S']$
Q, q	Taq polymerase, $q = [Q]$
C, c	complex of primed ssDNA with Taq, $c = [C]$
C_j, c_j	complex with j base pairs added, $j = 1, 2, ..., n, c_j = [C_j]$
R, r	resources containing nucleotides for extension, $r = [R]$
k_1, k_{-1}	forward and backward reaction rates for annealing
$\lambda_1, \lambda_2, \lambda_3$	forward reaction rates for extension stage
$\hat{s}$	initial amount of ssDNA for a single cycle
$\hat{p}$	initial amount of primer for a single cycle
$\hat{s}'$	initial amount of primed ssDNA for a single cycle
$\hat{q}$	initial amount of Taq for a single cycle
$\hat{r}$	initial amount of resources containing the individual base pairs
τ	rescaled time for extension stage ($\lambda_2 \hat{r} t$)
$\bar{s}$, $\bar{q}$, etc.	rescaled reactants for extension stage
ϵ	$\frac{\lambda_1 \hat{q}}{\lambda_2 \hat{r}}$, rate of Taq attachment relative to rate of extension
ν	$\frac{\lambda_1 \hat{p}}{\lambda_2 \hat{r}}$
μ	$\frac{\lambda_3}{\lambda_2 \hat{r}}$, rate of Taq detachment relative to rate of extension, $O(1)$

TABLE 1. List of variables and constants used in PCR model.

amount of ssDNA after dissociation), and $p(0) = \hat{p}$ (the amount of primer at the beginning of this stage). It can be observed from equations (1)-(3) that $\frac{ds}{dt} + \frac{ds'}{dt} = 0$ and $\frac{dp}{dt} + \frac{ds'}{dt} = 0$. This gives rise to two conserved quantities:

$$s + s' = K_1 = s(0) + s'(0) = s(0) = \hat{s},$$

and

$$p + s' = K_2 = p(0) + s'(0) = p(0) = \hat{p}.$$

Using these quantities the system can be reduced to a single equation,

$$\frac{ds'}{dt} = k_1(\hat{p} - s')(\hat{s} - s') - k_{-1}s', \tag{4}$$

and solved analytically, using separation of variables. The solution is

$$s'(t) = \frac{\alpha_+ \alpha_- (1 - e^{(\alpha_- - \alpha_+)t})}{\alpha_+ - \alpha_- e^{(\alpha_- - \alpha_+)t}}, \tag{5}$$

where

$$\alpha_\pm = \frac{k_{-1} + k_1\hat{p} + k_1\hat{s} \pm \sqrt{(k_{-1} + k_1\hat{p} + k_1\hat{s})^2 - 4k_1^2\hat{p}\hat{s}}}{2k_1}. \tag{6}$$

The sigmoidal solution (5) increases to a limiting quantity determined by the initial amounts of ssDNA and primer.

The solutions for primer and single-stranded DNA come from the conserved quantities and are:

$$s(t) = \hat{s} - s'(t) \tag{7}$$

and

$$p(t) = \hat{p} - s'(t). \tag{8}$$

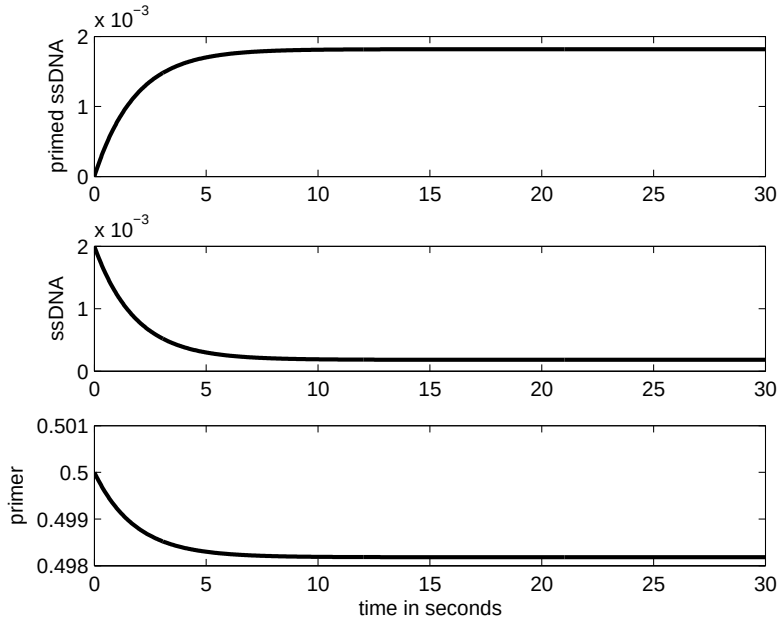

FIGURE 1. The graphs of the exact solutions for the annealing stage of a single cycle of PCR with $\hat{p} = .5$ and $\hat{s} = .002$. The rate constants used are $k_1 = 0.205$ and $k_{-1} = 0.01025$. The solution curve for primed ssDNA levels off when all of the ssDNA strands have been primed.

A graph of this solution is shown in Figure 1.

3.2. **Extension.** The law of mass action is again applied to write differential equations (9)-(16) that describe the change in concentration of each of the reactants as Taq extends the template copy. The constants, λ_1,λ_2, and λ_3 are forward reaction rates for this stage. The change in the concentration of primed ssDNA is proportional to the product of the concentrations of primed ssDNA, s', and unattached Taq, q, as shown in the equation,

$$\frac{ds'}{dt} = -\lambda_1 s' q. \tag{9}$$

The change in the concentration of unattached Taq is also a function of s' and q as well as the concentration of the complex with all the base pairs added, c_n. This models Taq binding with the primed ssDNA at the beginning of extension and detaching after the template strand is completed, giving

$$\frac{dq}{dt} = -\lambda_1 s' q + \lambda_3 c_n. \tag{10}$$

The change in the concentration of the complex, c, is a function of s', q, c, and the concentration of resources, r,

$$\frac{dc}{dt} = \lambda_1 s' q - \lambda_2 r c. \tag{11}$$

The next $n-1$ equations, represented by (12) and (13), exhibit a distinct pattern as they model addition of base pairs to the template strand. The pattern models the creation of the complex, C_j as the jth base pair is added to the previous complex, C_{j-1}, and its subsequent disappearance when the next base pair is added. The change in the concentration for a particular complex with j base pairs added is a function of the concentration of that complex, c_j, r, and the concentration of the previously formed complex, c_{j-1}.

$$\frac{dc_1}{dt} = \lambda_2 rc - \lambda_2 rc_1 \tag{12}$$

$$\vdots$$

$$\frac{dc_{n-1}}{dt} = \lambda_2 rc_{n-2} - \lambda_2 rc_{n-1}. \tag{13}$$

The equation for the change in the concentration of the complex with n base pairs differs from (12)-(13) and is written,

$$\frac{dc_n}{dt} = \lambda_2 c_{n-1} r - \lambda_3 c_n. \tag{14}$$

It is a function of the concentrations of the previous complex, c_{n-1}, r, and itself, c_n, but it includes λ_3, the rate at which Taq detaches from the completed complex, C_n, forming dsDNA. The change in the concentration of resources is affected by the concentrations of all the complexes up to c_{n-1} as shown in the equation,

$$\frac{dr}{dt} = -\lambda_2 r \sum_{j=1}^{n-1} c_j. \tag{15}$$

The change in the concentration of dsDNA is proportional to the concentration of the complex with all of the base pairs added, c_n:

$$\frac{dd}{dt} = \lambda_3 c_n. \tag{16}$$

The equation for double-stranded DNA, (16), is coupled only to (14) and can be solved by direct integration after (9)-(15) are solved. The initial conditions are: $s'(0) = \hat{s}'$ (the amount of primed ssDNA present at the end of the previous annealing stage), $q(0) = \hat{q}$ (the initial amount of Taq), $c(0) = c_j(0) = d(0) = 0$ (since dissociation peels off any partially competed amplicon), and $r(0) = \hat{r}$ (the amount of resources remaining after the previous extension stage).

An inherent small quantity in this stage of the PCR process is the proportion of the initial amount of Taq to the initial amount of resources, $\frac{\hat{q}}{\hat{r}}$, due to the fact that nucleotide base pairs are relatively easier to obtain and used in much larger quantities than Taq, which is relatively rare and expensive. Therefore we choose a time scale and concentration scales to form a dimensionless system in a way that lets us take advantage of this small quantity. This amounts to assuming that Taq is the rate-limiting quantity. The time is non-dimensionalized using $\tau = \lambda_2 \hat{r} t$, and the concentrations are normalized using: $\bar{s}' = \frac{s'}{\hat{p}}$, $\bar{q} = \frac{q}{\hat{q}}$, $\bar{c} = \frac{c}{\hat{q}}$, $\bar{c}_j = \frac{c_j}{\hat{q}}$, and , $\bar{r} = \frac{r}{\hat{r}}$.

Using dot notation for $\frac{d}{d\tau}$ ($\frac{d\bar{s}'}{d\tau} = \dot{\bar{s}}'$, etc.), the equations (9)-(15) become:

$$\dot{\bar{s}}' = -\frac{\lambda_1 \hat{q}}{\lambda_2 \hat{r}} \bar{s}' \bar{q}, \tag{17}$$

$$\dot{\bar{q}} = -\frac{\lambda_1 \hat{p}}{\lambda_2 \hat{r}} \bar{s}' \bar{q} + \frac{\lambda_3}{\lambda_2 \hat{r}} \bar{c}_n, \tag{18}$$

$$\dot{\bar{c}} = \frac{\lambda_1 \hat{p}}{\lambda_2 \hat{r}} \bar{s}' \bar{q} - \bar{r}\bar{c}, \tag{19}$$

$$\dot{\bar{c}}_1 = \bar{r}\bar{c} - \bar{r}\bar{c}_1, \tag{20}$$

$$\vdots$$

$$\dot{\bar{c}}_{n-1} = \bar{r}\bar{c}_{n-2} - \bar{r}\bar{c}_{n-1}, \tag{21}$$

$$\dot{\bar{c}}_n = \bar{r}\bar{c}_{n-1} - \frac{\lambda_3}{\lambda_2 \hat{r}} \bar{c}_n, \tag{22}$$

and

$$\dot{\bar{r}} = -\frac{\hat{q}}{\hat{r}} \bar{r} \sum_{j=1}^{n-1} \bar{c}_j, \tag{23}$$

with rescaled initial conditions $\bar{s}'(0) = \frac{\hat{s}'}{\hat{p}} = \gamma$, $\bar{q}(0) = \frac{\hat{q}}{\hat{q}} = 1$, $\bar{r}(0) = \frac{\hat{r}}{\hat{r}} = 1$,and $\bar{c}(0) = \bar{c_j}(0) = 0$.

The quantity $\frac{\lambda_1 \hat{q}}{\lambda_2 \hat{r}}$ in (17), contains the small quantity, $\frac{\hat{q}}{\hat{r}}$. Since the rate constants, λ_1 and λ_2 are of the same order, $\epsilon = \frac{\lambda_1 \hat{q}}{\lambda_2 \hat{r}}$ is small. We define two other dimensionless parameters, $\nu = \frac{\lambda_1 \hat{p}}{\lambda_2 \hat{r}}$, and $\mu = \frac{\lambda_3}{\lambda_2 \hat{r}}$ for simplification. The system (17)-(23) becomes:

$$\dot{\bar{s}}' = -\epsilon \bar{s}' \bar{q}, \tag{24}$$

$$\dot{\bar{q}} = -\nu \bar{s}' \bar{q} + \mu \bar{c}_n, \tag{25}$$

$$\dot{\bar{c}} = \nu \bar{s}' \bar{q} - \bar{r}\bar{c}, \tag{26}$$

$$\dot{\bar{c}}_1 = \bar{r}\bar{c} - \bar{r}\bar{c}_1 \tag{27}$$

$$\vdots$$

$$\dot{\bar{c}}_{n-1} = \bar{r}\bar{c}_{n-2} - \bar{r}\bar{c}_{n-1}, \tag{28}$$

$$\dot{\bar{c}}_n = \bar{r}\bar{c}_{n-1} - \mu \bar{c}_n, \tag{29}$$

and

$$\dot{\bar{r}} = -\epsilon \frac{\lambda_2}{\lambda_1} \bar{r} \sum_{j=1}^{n-1} \bar{c}_j. \tag{30}$$

3.3. **Multiple time scale analysis.** The presence of a small parameter, ϵ, allows the application of the method of multiple time scales. A more detailed description of this method is found in Holmes [3]. This small parameter, calculated using parameters derived from the literature [5], [17], is of order 10^{-4}. The details of the parameter derivations are found in the multi-cycle map section. Assigning $t_1 = \tau$ to be the fast time scale and $t_2 = \epsilon\tau$ to be the slow time scale, $\frac{d}{d\tau}$ becomes $\frac{\partial}{\partial t_1} + \epsilon \frac{\partial}{\partial t_2} = \partial_{t_1} + \epsilon \partial_{t_2}$. We substitute this new time derivative into equations (24)-(30), along with a power series expansion of the form

$$y = y_0(t_1, t_2) + \epsilon y_1(t_1, t_2) + ..., \tag{31}$$

Symbol	Units	Value
$\hat{p}$	μmol μl^{-1}	0.5
$\hat{q}$	μmol μl^{-1}	0.01
$\hat{r}$	μmol μl^{-1}	20
k_1	μl μmol^{-1} sec^{-1}	0.205
k_{-1}	sec^{-1}	0
λ_1	μl μmol^{-1} sec^{-1}	9
λ_2	μl μmol^{-1} sec^{-1}	10
λ_3	sec^{-1}	100

TABLE 2. Parameters in PCR model and their values used in simulations. Parameter estimates are based on published data and/or experimental protocol corresponding to the graph of PCR data shown in Figure 3. These parameters generate $\epsilon = 4.5 \times 10^{-4}$. Concentrations are in micromoles per microliter (μmol μl^{-1}) and time is in seconds.

for each concentration variable. For example, (24) becomes

$$(\partial_{t_1} + \epsilon\partial_{t_2})(\bar{s}_0' + \epsilon\bar{s}_1' + ...) = -\epsilon(\bar{s}_0' + \epsilon\bar{s}_1' + ...)(\bar{q}_0 + \epsilon\bar{q}_1 + ...). \tag{32}$$

Collecting the order ϵ^0 terms gives the leading order equations:

$$\partial_{t_1}\bar{s}_0' = 0, \tag{33}$$
$$\partial_{t_1}\bar{q}_0 = -\nu\bar{s}_0'\bar{q}_0 + \mu\bar{c}_{n_0}, \tag{34}$$
$$\partial_{t_1}\bar{c}_0 = \nu\bar{s}_0'\bar{q}_0 - \bar{r}_0\bar{c}_0, \tag{35}$$
$$\partial_{t_1}\bar{c}_{1_0} = \bar{r}_0\bar{c}_0 - \bar{r}_0\bar{c}_{1_0}, \tag{36}$$
$$\partial_{t_1}\bar{c}_{2_0} = \bar{r}_0\bar{c}_{1_0} - \bar{r}_0\bar{c}_{2_0}, \tag{37}$$
$$\vdots$$
$$\partial_{t_1}\bar{c}_{n-1_0} = \bar{r}_0\bar{c}_{n-2_0} - \bar{r}_0\bar{c}_{n-1_0}, \tag{38}$$
$$\partial_{t_1}\bar{c}_{n_0} = \bar{r}_0\bar{c}_{n-1_0} - \mu\bar{c}_{n_0}, \tag{39}$$

and

$$\partial_{t_1}\bar{r}_0 = 0. \tag{40}$$

The initial conditions become: $\bar{s}_0'(t_1 = t_2 = 0) = \gamma$, $\bar{q}_0(t_1 = t_2 = 0) = \bar{r}_0(t_1 = t_2 = 0) = 1$, and $\bar{c}_0(t_1 = t_2 = 0) = \bar{c}_{j_0}(t_1 = t_2 = 0) = 0$.

Equations (33) and (40) imply that $\bar{r}_0$ and $\bar{s}_0'$ are constant on the fast time scale. This means that the system of equations(34)-(39), is linear and can be written in vector form as

$$\boldsymbol{x}'(t_1) = A\boldsymbol{x}(t_1),$$

where A is the coefficient matrix. The sum of the rows of A equals zero, and it is easy to show that A has one zero eigenvalue and $n+1$ eigenvalues less than zero. Therefore the solution for this linear system takes the form,

$$\boldsymbol{x}(t_1) = \boldsymbol{v}_0 + \sum_{j=1}^{n} e^{\xi_j t_1}\boldsymbol{v}_j,$$

where $\boldsymbol{v}_0$ is an eigenvector associated with the zero eigenvalue, and the ξ_j's are eigenvalues with negative real parts, with their associated eigenvectors, $\boldsymbol{v}_j$. Consequently, $\boldsymbol{x}(t_1) \to \boldsymbol{v}_0$ exponentially fast on the fast time scale. Ignoring these transients, the leading order solution becomes $\boldsymbol{x}(t_1) = \boldsymbol{v}_0$.

With the above in mind, we determine $\boldsymbol{v}_0$ using the conserved quantity obtained by adding together the right sides of (34)-(39),

$$\bar{q}_0 + \bar{c}_0 + \sum_{j=1}^{n-1} \bar{c}_{j_0} = K = \bar{q}_0(0) + \bar{c}_0(0) + \sum_{j=1}^{n-1} \bar{c}_{j_0}(0) = 1. \tag{41}$$

$K = 1$ is determined using the initial conditions. Solving $\bar{q}_0 + \bar{c}_0 + \sum_{j=1}^{n-1} \bar{c}_{j_0} = 1$ for $\bar{q}_0$ yields,

$$\bar{q}_0 = 1 - \bar{c}_0 - \sum_{j=1}^{n-1} \bar{c}_{j_0}. \tag{42}$$

Setting the right hand sides of (35)-(39) to zero and solving yields:

$$\bar{c}_{n_0} = \frac{\nu \bar{s}_0'}{\mu} \bar{q}_0, \tag{43}$$

$$\bar{c}_0 = \nu \bar{s}_0' \bar{q}_0, \tag{44}$$

and

$$\bar{c}_0 = \bar{c}_{1_0} = \bar{c}_{2_0} = \cdots = \bar{c}_{n-1_0}. \tag{45}$$

Using (43)-(45), the equation for $\bar{q}_0$, (42), becomes

$$\bar{q}_0 = \frac{\mu}{\mu + n\mu\nu\bar{s}_0' + \nu\bar{s}_0'}, \tag{46}$$

where n, the number of base pairs added, acts as a shape parameter.

The order ϵ^1 equation for $\bar{s}'$ is

$$\partial_{t_1} \bar{s}_1' = -\bar{s}_0' \bar{q}_0 - \partial_{t_2} \bar{s}_0'. \tag{47}$$

Solving this equation yields:

$$\bar{s}_1' = -(\bar{s}_0' \bar{q}_0 + \partial_{t_2} \bar{s}_0') t_1, \tag{48}$$

since $\bar{s}_0'$ and $\bar{q}_0$ are functions only of t_2. To eliminate the secular term in (48), we require

$$0 = \partial_{t_2} \bar{s}_0' + \bar{s}_0' \bar{q}_0 = \partial_{t_2} \bar{s}_0' + \frac{\mu \bar{s}_0'}{\mu + n\mu\nu\bar{s}_0' + \nu\bar{s}_0'} = 0, \tag{49}$$

using the expression for $\bar{q}_0$ in (46). We solve (49) using separation of variables. Separating and integrating gives

$$\mu \ln \bar{s}_0' + (n\mu + 1)\nu\bar{s}_0' = -\mu t_2 + K, \tag{50}$$

where K is an integration constant. The initial condition $\bar{s}_0'(t_2 = 0) = \gamma$ gives

$$K = \mu \ln \gamma + (n\mu + 1)\nu\gamma.$$

The implicit solution for $\bar{s}_0'$, (50), becomes

$$\mu \ln \bar{s}_0' + (n\mu + 1)\nu\bar{s}_0' = -\mu t_2 + \mu \ln \gamma + (n\mu + 1)\nu\gamma,$$

which can be solved for t_2,

$$t_2 = \frac{\mu \ln \bar{s}_0' - (n\mu + 1)\nu\bar{s}_0' + \mu \ln \gamma + (n\mu + 1)\nu\gamma}{\mu}. \tag{51}$$

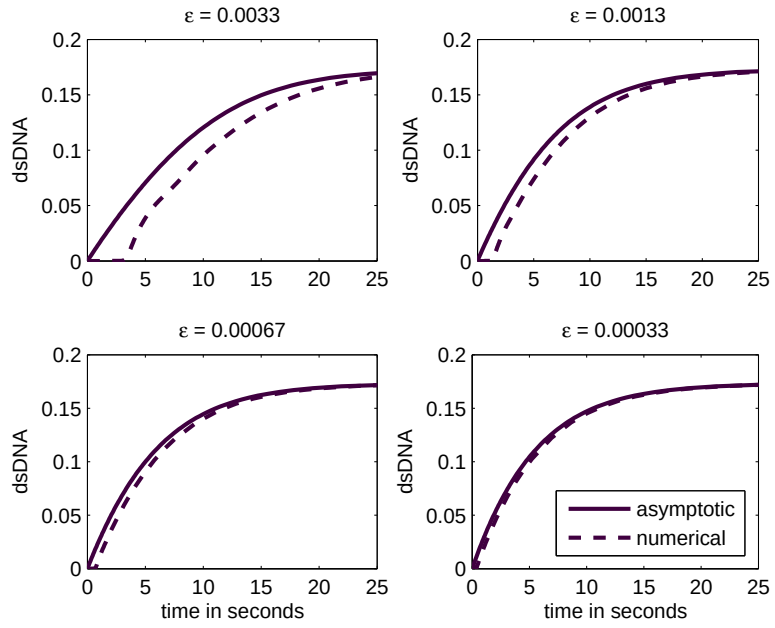

FIGURE 2. Comparison of asymptotic (solid lines) and numerical (dashed lines) solutions for dsDNA in the extension stage for various values of ϵ with a target strand length of $n = 200$. A Runge-Kutta method was used to generate the numerical solutions. As ϵ tends towards zero, the asymptotic and numerical solutions converge.

Returning to the original scale, equations (51) and (43)-(46) become:

$$t = \frac{\ln \frac{\hat{s'}}{s'}}{\epsilon\lambda_2\hat{r}} + \frac{\nu(n\mu+1)(\hat{s'}-s')}{\mu\epsilon\lambda_2\hat{r}\hat{p}}, \tag{52}$$

$$q = \frac{\mu\hat{q}\hat{p}}{\mu\hat{p}+n\mu\nu s'+\nu s'}, \tag{53}$$

$$c_n = \frac{\nu\hat{q}s'}{\mu\hat{p}+n\mu\nu s'+\nu s'}, \tag{54}$$

$$c = c_1 = c_2 = \cdots = c_{n-1} = \mu c_n. \tag{55}$$

The solution to our original equation for double-stranded DNA is

$$d = \lambda_3 \int_0^{t_{end}} c_n(t)dt. \tag{56}$$

The units used in the original scale are shown in Table 2.

Figure 2 shows a comparison between the asymptotic and numerical solutions for the concentration of dsDNA in the extension stage. A Runge Kutta method was used for the numerical solution. The asymptotic and numerical solutions converge as ϵ tends towards zero.

4. **Multi-cycle map.** A map from one cycle of PCR to the next can be constructed from the solutions for the annealing and extension stages and their initial conditions. This is done by cascading the results of a previous cycle into the initial conditions for the next cycle. Let the concentration of primed ssDNA be represented by s'^A for the annealing stage and by s'^E for the extension phase. Also, let the final times for the annealing and extension stages be fixed at t_A and t_E respectively.

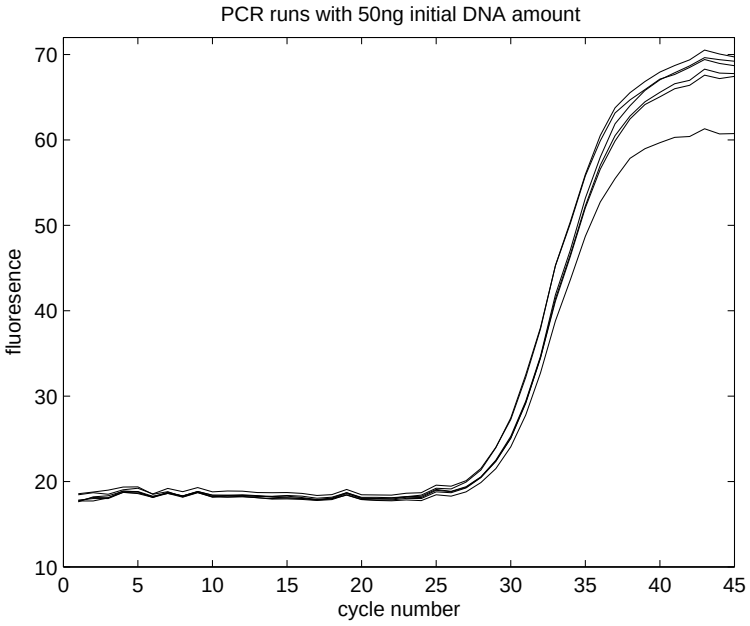

FIGURE 3. The fluorescence data from a dilution series with a 50ng initial DNA sample and a 107 base pair product provided by Idaho Technology Inc.

The first cycle begins with initial amounts of resources, primer and Taq, and a sample containing the dsDNA to be duplicated. For our simulations we used initial amounts for resources, primer and Taq provided by Idaho Technology Inc. for a typical rapid PCR. The amounts for resources and primer are listed in Table 2. Taq was given in terms of a unit, defined as the amount of enzyme that incorporates 10 nanomoles of nucleotide base pairs into acid-precipitable material in 30 minutes at 74^{o}C [5]. To convert a unit into micromoles per microliter, we consider the relationship,

$$q\lambda_2 t_E N = bp_{total},$$

where q is the number of Taq molecules, N is the number of cycles, and bp_{total} number of base pairs. If we require this to equal the limiting value, $p(0) \times n$, where n is the number of base pairs per amplicon, we can solve for the amount of Taq. The amount of resources, $\hat{r}$, is considered as essentially constant in the map; the amount of resource used is too small to have an appreciable effect.

Assuming that dissociation is complete, the initial amount of ssDNA for the annealing stage of the first cycle is $s_1(0) = 2d_1$. The other initial conditions for the annealing stage of the first cycle are $p_1(0) = \hat{p}$ (the amount of primer at the

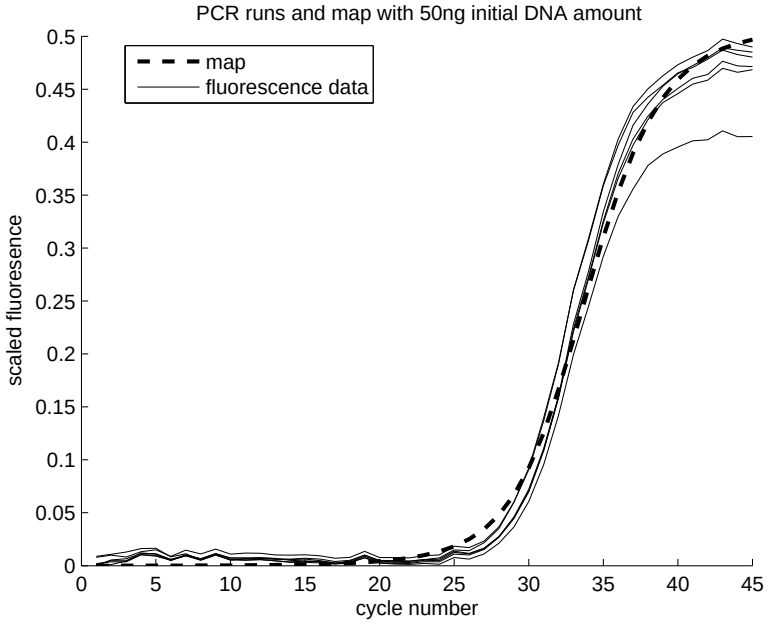

FIGURE 4. A comparison of the fluorescence data with the map, using similar initial amounts and dissociation and extension times. The fluorescence level has been scaled according to a linear relationship with the concentration of dsDNA produced.

beginning of the PCR run) and $s_1'^A(0) = 0$. For all other cycles dissociation not only denatures the dsDNA created in the extension phase, it also denatures any primed ssDNA and any complexes that remain after extension. Thus, for the annealing stage of the ith cycle, the initial amount of ssDNA, $s_i(0)$, includes not only twice the amount of dsDNA from the previous cycle, but also the amount of ssDNA, the amounts of primed ssDNA, and the amount of all of the complexes from the previous cycle. This can be written as

$$\begin{aligned} s_i(0) = 2d_{i-1}(t_E) + s_{i-1}(t_A) + s_{i-1}'^E(t_E) + c_{i-1}(t_E) \\ + c_{1\,i-1}(t_E) + \ldots + c_{n-1\,i-1}(t_E) + c_{n\,i-1}(t_E). \end{aligned}$$

Likewise, the initial amount of primer for the ith cycle is the sum of the amount of primer from the previous cycle plus the primers gained from denaturing the primed ssDNA and the complex of Taq and primed ssDNA from the previous cycle, written as,

$$p_i(0) = p_{i-1}(t_A) + s_{i-1}'^E(t_E) + c_{i-1}(t_E).$$

The initial condition for primed ssDNA is $s_i'^A(0) = 0$, because dissociation is assumed to be complete. This model does not keep track of any incomplete product accumulating from cycle to cycle.

Then using solutions (5)-(8), the map for the annealing stage of the ith cycle is:

$$s_i'^A(t_A) = \frac{\alpha_+\alpha_-(1 - e^{(\alpha_- - \alpha_+)t_A})}{\alpha_+ - \alpha_- e^{(\alpha_- - \alpha_+)t_A}},$$

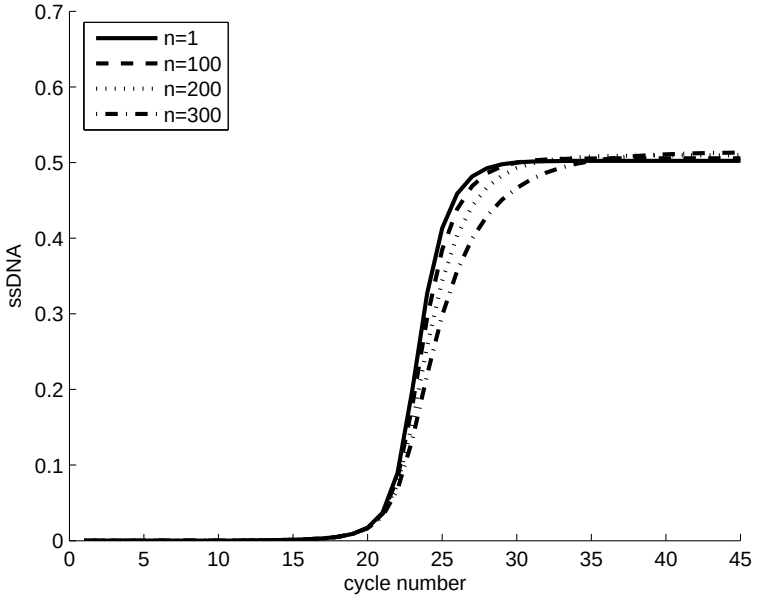

FIGURE 5. The PCR map for various lengths of target DNA. The longer the target strand, the longer it takes the solution to reach a limiting value. Thus, n acts as a shape parameter.

where

$$\alpha_{\pm} = \frac{k_{-1} + k_1 p_i(0) + k_1 s_i(0) \pm \sqrt{(k_{-1} + k_1 p_i(0) + k_1 s_i(0))^2 - 4k_1^2 p_i(0) s_i(0)}}{2k_1},$$

$$s_i(t_A) = s_i(0) - s_i'^A(t_A),$$

and

$$p_i(t_A) = p_i(0) - s_i'^A(t_A).$$

The values for the rate constants, k_1 and k_{-1} used in our simulations are given in Table 2. They were fit to data provided by Idaho Technology Inc. during a previous research project [8].

The amount of primed ssDNA at the beginning of extension stage for the ith cycle is the amount at the end of the annealing stage of that same cycle, $s_i'^E(0) = s_i'^A(t_A)$. The initial amount of Taq is the beginning amount for the first cycle, $q_1 = \hat{q}$ and the amount from the previous cycle for the rest of the cycles, $q_i(0) = q_{i-1}(t_E)$. The initial conditions for dsDNA and all the complexes for the extension stage of the ith cycle are: $c_i(0) = c_{1i}(0) = c_{2i}(0) = \cdots = c_{ni}(0) = 0$ and $d_i(0) = 0$, because dissociation is assumed to be complete.

A map for the extension stage can be derived from the solutions (51)-(55). The value for $s_i'^E(t_E)$ is extracted numerically from the implicit relationship

$$t_E = \frac{\ln \frac{s_i'^E(0)}{s_i'^E(t_E)}}{\epsilon \lambda_2 \hat{r}} + \frac{\nu(n\mu + 1)(s_i'^E(0) - s_i'^E(t_E))}{\mu \epsilon \lambda_2 \hat{r} p_i(0)}.$$

The concentrations for the rest of the reactants are given by:

$$q_i = \frac{\mu q_i(0) p_i(0)}{\mu p_i(0) + n\mu\nu s_i'^E(t_E) + \nu s_i'^E(t_E)},$$
$$c_{ni} = \frac{\nu q_i(0) s_i'^E(t_E)}{\mu p_i(0) + n\mu\nu s_i'^E(t_E) + \nu s_i'^E(t_E)},$$
$$c_i(t_E) = c_{1i}(t_E) = c_{2i}(t_E) = \cdots = c_{n-1i}(t_E) = \mu c_{ni}(t_E),$$

and

$$d_i(t_E) = \int_0^{t_E} \lambda_3 c_{ni}(s) ds.$$

The equation for $d_i(t_E)$ is solved numerically, using trapezoidal quadrature.

At 72^oC Taq Polymerase has an extension rate of 35-100 nucleotides per second [17]. Using an extension rate of 40 nucleotides per second, we estimated the value of the rate constant λ_2,

$$\lambda_2 \sim \frac{40\text{bp/sec}}{4\mu\text{M}/\mu\text{l}} = 10.$$

The rate constants λ_1 and λ_3 were then chosen in relationship to λ_2. λ_1 was chosen assuming a similar rate for adding Taq to the primed ssDNA as adding base pairs. λ_3 was chosen so that the proportion $\frac{\lambda_3}{\lambda_2 R}$ is $O(1)$.

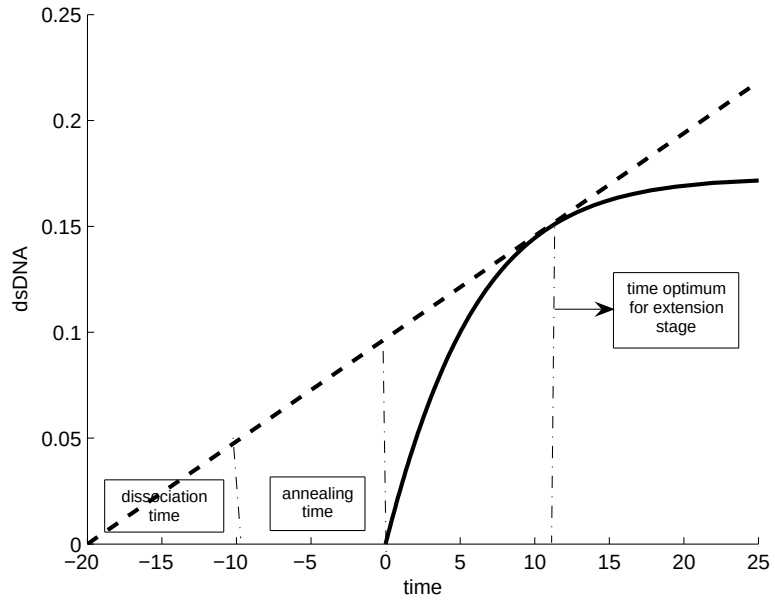

FIGURE 6. An illustration of the idea of optimization. The solid curved graph represents the solution for the extension stage for $n = 200$. The negative part of the time axis represents the time spent in the preceding dissociation and annealing stages. The tangent line touches the solid curve at the point of the optimal time to run the extension phase.

The behavior of the solutions can be explored by using this map to simulate the PCR process. The fluorescence data from a dilution series with a 50ng initial DNA sample and a 107 base pair product provided by Idaho Technology Inc. is shown in Figure 3. A comparison of this data with the map, using similar initial amounts and dissociation and extension times, is shown in Figure 4. In order for the fluorescence data to be compared with the map, a linear relationship between the concentration of DNA and the fluorescence level was assumed. The measured fluorescence was scaled to have a maximum value equal to the initial primer amount since the initial primer amount limits the amount of dsDNA produced. The background fluorescence, which is not modeled by the map, was removed. Figure 5 shows graphs of the map with varying lengths of target DNA.

5. **Optimization.** This model and its approximate map may be used to optimize the process in order to produce the most DNA copies in the shortest amount of time possible. Since we don't know the concentration of dsDNA during the reaction, and in fact the amount will vary from sample to sample, we choose to optimize time independent of the initial dsDNA concentration at the beginning of each cycle. Let d_{total} be the total dsDNA produced by a PCR in N cycles and t_c be the time required per cycle. Then by the following relationship,

$$d_{total} = d(N) - d(0) = \int_0^{Nt_c} \frac{dd}{dt} dt \approx \sum_{i=1}^{N} \frac{\Delta d(i)}{t_c},$$

maximizing the change in dsDNA concentration per time for each individual cycle maximizes the total amount of dsDNA produced in the shortest amount of time. For an example of how this might be done, we consider optimizing the time spent in the extension stage of a cycle. Let t_D and t_A be the fixed times for the dissociation and annealing stages, respectively. Let t be the variable representing the time spent in the extension stage. Then the total time to complete one cycle of PCR is $t_c = t_D + t_A + t$. Let $d(t)$ be the total amount of dsDNA produced in a PCR cycle. Then the t such that

$$\frac{d}{dt}\left(\frac{d(t)}{t_D + t_A + t}\right) = 0,$$

is the optimal time for the extension stage for one cycle, corresponding to maximizing the rate amplicon is produced during this cycle in the context of the iterated map. Thus the optimal extension time is expected to change from cycle to cycle as the capacity to produce amplicon changes. Differentiating,

$$\frac{d}{dt}\left(\frac{d(t)}{t_D + t_A + t}\right) = \frac{d'(t)}{t_D + t_A + t} - \frac{d(t)}{(t_D + t_A + t)^2}. \tag{57}$$

Setting the right hand side of (57) equal to zero gives us

$$d'(t) = \frac{d(t)}{t_D + t_A + t}. \tag{58}$$

Graphically this can be viewed as finding the point on the graph of $d(t)$ at which the rate of production(the left hand side of (58)) is equal to the slope of a secant line (right hand side of (58)) connecting the graph and the point $d = 0$, $t = -(t_D + t_A)$, as illustrated in Figure 6. Then using the right sides of equations (16) and (56) for

$d'(t)$ and $d(t)$, (58) becomes

$$(t_D + t_A + t)\lambda_3 c_n = \lambda_3 \int_0^t c_n(s)ds. \tag{59}$$

After simplification we have

$$(t_D + t_A + t)c_n = \int_0^t c_n(s)ds. \tag{60}$$

The t that makes (60) true is found numerically by using the solutions for the extension stage. In order to produce the most dsDNA over the shortest amount of time for an entire PCR run, we include the optimization for the extension stage in the map. The optimal time is calculated and used for each iteration of the extension stage. A set time is used for all the iterations of the annealing stage.

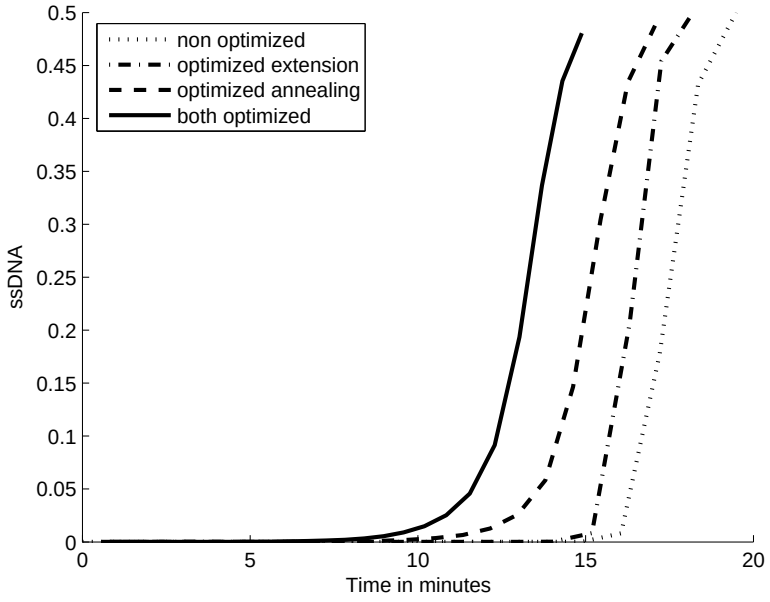

FIGURE 7. A comparison of optimized runs to a run with a fixed annealing and extension stage times of 20 and 30 seconds. Each run has simulation amplicon length of $n = 200$. Parameters were chosen based on published data and Idaho Technology experimental protocols cited in the text and summarized in Table 2.

A similar optimization can be performed for the annealing stage to obtain the most primed ssDNA in the shortest time possible. A comparison of optimizing the extension stage only, optimizing the annealing stage only, and optimizing both to using fixed annealing and extension times, 20 and 30 seconds, respectively, is shown in Figure 7. This graph shows the amplification profile for a target strand length of $n = 200$. These results show that optimizing the annealing stage may reduce

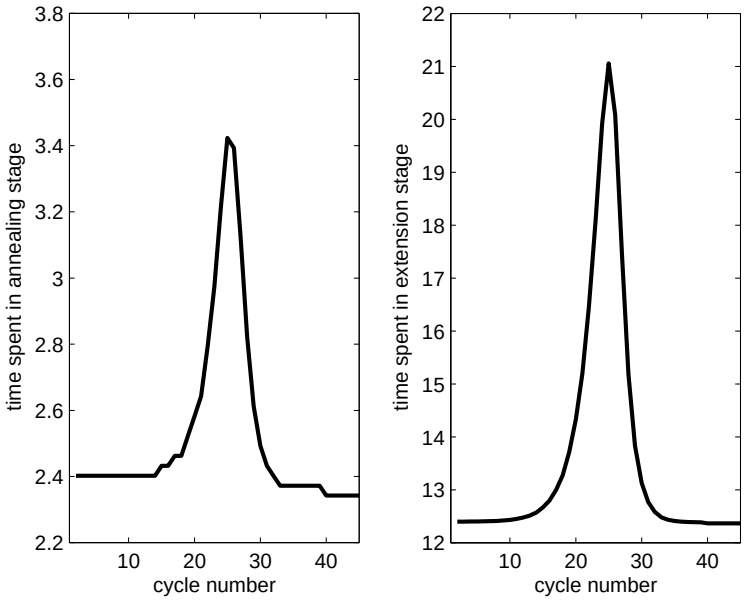

FIGURE 8. The time spent in the annealing and extension stages for each cycle for a run with both stages optimized. The optimal time changes dynamically with the amount of product being produced. Notice that before and after the spike around the 25th cycle, the optimal time settles to a constant base value.

the time for a PCR run more than just optimizing the extension stage. The time spent in the annealing and extension stages for each cycle for a run with both stages optimized is shown in Figure 8.

The graph on the right in Figure 8 shows the times for the optimized extension times, allowing a longer extension time in the middle of the PCR process when more product is being produced. It is quite noticeable that there exists a base optimal time for extension on either side of the peak for the early and ending cycles of the process. If this base optimal time could be predicted analytically, it would be 'almost optimal' and much simpler to implement. We observe that the amount of primed ssDNA is small in the early and ending cycles of a PCR. Assuming a small s' allows us to neglect the second term in (52), and neglect terms involving s' in the denominators of (53) and (54), leaving

$$t = \frac{\ln \frac{\hat{s}'}{s'}}{\epsilon \lambda_2 \hat{r}}, \tag{61}$$

$$q = \frac{\mu \hat{q} \hat{p}}{\mu \hat{p}} = \hat{q}, \tag{62}$$

and

$$c_n = \frac{\nu \hat{q} s'}{\mu \hat{p}}. \tag{63}$$

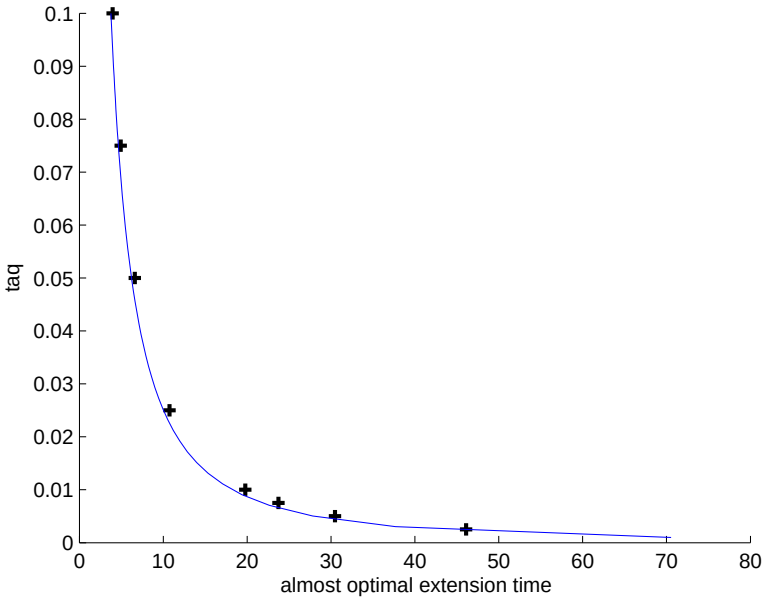

FIGURE 9. The data points represent the base extension stage times for various initial amounts of Taq, using the fully optimized extension stage map. The curve shows the relationship between initial amounts of Taq and the almost optimal extension time as calculated by (68).

Solving for s' in (61) gives

$$s' = \hat{s}' e^{-\epsilon\lambda_2 \hat{r} t}. \tag{64}$$

Substituting (64) into (63) yields

$$c_n = \frac{\nu \hat{q} \hat{s}' e^{-\epsilon\lambda_2 \hat{r} t}}{\mu \hat{p}}. \tag{65}$$

This expression for c_n can be substituted into (60) giving

$$(t_D + t_A + t)\frac{\nu \hat{q} \hat{s}' e^{-\epsilon\lambda_2 \hat{r} t}}{\mu \hat{p}} = \int_0^t \frac{\nu \hat{q} \hat{s}' e^{-\epsilon\lambda_2 \hat{r} s}}{\mu \hat{p}} ds.$$

Integrating and simplifying yields a relationship that the optimal base extension time satisfies,

$$\frac{1 - e^{-\epsilon\lambda_2 \hat{r} t}}{t_D + t_A + t} = e^{\epsilon\lambda_2 \hat{r} t}. \tag{66}$$

Using the definition, $\epsilon = \frac{\lambda_1 \hat{q}}{\lambda_2 \hat{r}}$,

$$\epsilon\lambda_2 \hat{r} = \lambda_1 \hat{q} \tag{67}$$

and (66) becomes

$$\frac{1 - e^{-\lambda_1 \hat{q} t}}{t_D + t_A + t} = e^{\lambda_1 \hat{q} t}. \tag{68}$$

The optimal base extension time depends on the initial amount of Taq, $\hat{q}$, and the rate that Taq binds to the primed ssDNA, λ_1. The relationship between the initial amount of Taq and the optimal base extension time is shown in Figure 9. This relationship closely follows the base optimal extension time computed by the PCR map with optimal extension. Figure 10 compares a non-optimized PCR run with a set extension time of 30 seconds with a run with optimized extension and a non-optimized PCR run using the optimal base extension time. Using the base extension time shortens the time required to achieve of a 90% of maximum yield similarly to using the map with optimized extension.

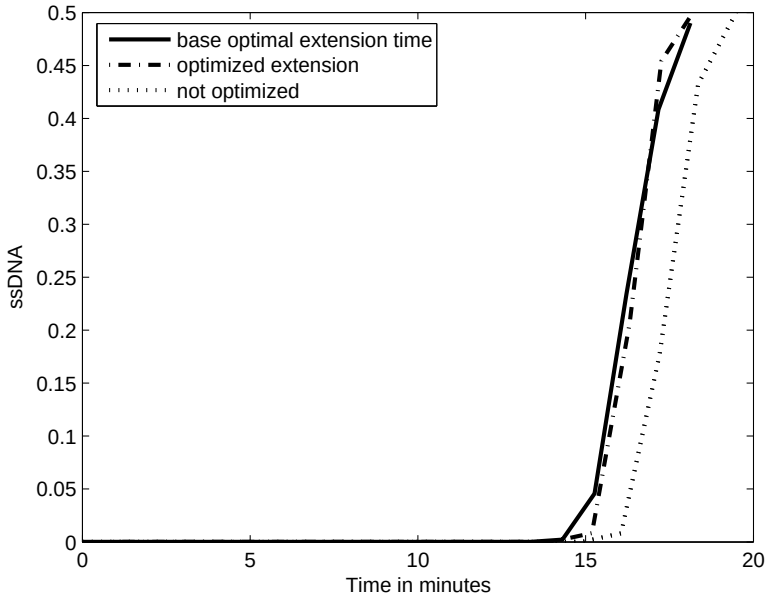

FIGURE 10. A comparison of a run with optimized extension stage to a non-optimized run with a fixed annealing and extension stage times of 20 and 30 seconds, respectively and a non-optimized run using the optimal base time for extension. Each run has a target strand length of $n = 200$. Parameters were chosen based on published data and Idaho Technology experimental protocols cited in the text and summarized in Table 2.

6. **Discussion and conclusion.** In this paper, we have described PCR, discussed existing models, and developed a model from the chemical equations using the law of mass action. This model of PCR is sensitive to the length of the target DNA strand and models the effect of strand length on the solution shape. We found a simple solution for the dissociation stage, analytical solutions for the annealing stage, and asymptotic approximations for the extension stage using the method of multiple scales. These solutions were put into a multi-cycle map to simulate PCR. The solutions and the map were then used to optimize the time spent in the extension and annealing stages of each cycle. The asymptotic solutions were also

used to find an almost optimal base extension time by its relationship with $\hat{q}$ and λ_1. This research suggests a way to calculate optimal extension times to potentially reduce the overall time for a PCR run.

This represents a potential breakthrough for real time application of PCR in time-critical circumstances. A limitation of the direct optimization described in this paper is that every sample undergoing amplification would require constant monitoring and individualized treatment. Since the individual treatment required would be differential exposure to temperatures in extension and annealing phases it is hard to imagine, practically, how this would be accomplished for large number of samples. Conversely, fully optimized treatment of single samples might have limited application for individual pathogen monitoring in on-site circumstances. A wide variety of interesting and useful rapid-PCR applications would be neglected, including multiplexed reactions (those amplifying more than one segment of DNA at a time) and multiple samples from differing sites/patients amplifying the same segments but at varying initial concentrations.

The beauty of the nearly optimal protocol is that its parameters depends *solely* on parameters which can easily be held constant across samples and within a multiplexed reaction: concentration of Taq, single nucleotide base pairs, and the rate at which Taq inserts new base pairs. The benefit of the asymptotic multi-scale analysis, based on the assumption that the reaction is generally saturated with single nucleotide base pairs and limited by availability of the (relatively expensive) Taq enzyme, is demonstrating that this near-optimization is in fact so universal. Practically speaking this is probably why PCR has worked as well as it has and why intuitive optimization of the reaction by practical chemical engineers has developed parameters very close to what we estimate here.

Acknowledgments. MJG was supported by a generous research grant from Idaho Technology Inc. during the spring and summer of 2006. Elements of the modeling were initially discussed with Emily Stone, University of Montana, whose insights were most helpful.

REFERENCES

[1] J. Aach and G. M. Church, *Mathematical models of diffusion-constrained polymerase chain reactions: Basis of high-throughput nucleic acid assays and simple self-organizing systems*, J. Theor. Biol., **228** (2004), 31–46.

[2] J. L. Gevertz, S. M. Dunn and C. M. Roth, *Mathematical model of real-time PCR kinetics*, Biotecnol. Bioeng., **92** (2005), 346–355.

[3] M. H. Holmes, "Introduction to Perturbation Methods," Springer-Verlag, New York, 1995.

[4] P. Jagers and F. Klebaner, *Random variation and concentration effects in PCR*, J. Theor. Biol., **224** (2003), 299–304.

[5] Invitrogen Life Technologies, "Manual: Platinum Taq DNA Polymerase," 2002.

[6] N. Lalam, *Estimation of the reaction efficiency in polymerase chain reaction*, J. Theor. Biol., **242** (2006), 947–953.

[7] W. Liu and D. A. Saint, *Validation of a quantitative method for real time PCR kinetics*, Biochem. Biophys. Res. Commun., **294** (2002), 347–353.

[8] A. Maw, "Polymerase Chain Reaction Thermal Protocol Optimization," Technical report for Idaho Tecnology Inc. 2006.

[9] C. Ramakers, J. M. Ruijter, R. H. Lekanne Deprez and A. F. M. Moorman, *Assumption-free analysis of quantitative real-time polymerase chain reaction (PCR) data*, Neuroscience Letters, **339** (2003), 62–66.

[10] R. G. Rutledge, *Sigmoidal curve-fitting redefines quantitative real-time PCR with the prospective of developing automated high-throughput applications*, Nucleic Acids Res., **32** (2004), e178.

[11] R. Saiki, S. Scharf, F. Faloona, K. Mullis, G. Horn and H. Erlich, *Enzymatic amplification of beta-globin genomic sequences and restriction site analysis for diagnosis of sickle cell anemia*, Science, **230** (1985), 1350–54.
[12] E. Stone, J. Goldes and M. Garlick, "A Multi-stage Model for Quantitative PCR," Technical report for Department of Mathematical Sciences, University of Montana.
[13] F. Sun, D. Galas, and M. Waterman, *A mathematical analysis of in vitro molecular selection-amplification*, J. Mol. Biol., **258** (1996), 650–660.
[14] M. A. Valasek and J. J. Repa, *The power of real-time PCR*, Advan. Physiol. Educ., **29** (2005), 151–159.
[15] M. Velikanov and R. Kapral, *Polymerase chain reaction: A Markov process approach*, J. Theor. Biol., **201** (1999), 239–249.
[16] G. Weiss and A. von Haeseler, *Modeling the polymerase chain reaction*, J. Comut. Biol., **2** (1995), 49–61.
[17] C. Wittwer and D. Garling, *Rapid Cycle DNA Amplification: Time and temperature optimization*, BioTechniques, **10** (1991), 76–83.

Received April 8, 2008; Accepted February 2, 2009.

E-mail address: marti.garlick@aggiemail.usu.edu
E-mail address: jim.powell@usu.edu
E-mail address: eyre@idahotech.com
E-mail address: tom_robbins@idahotech.com